

# Role of the Mineral in the Self-Healing of Cracks in Human Enamel

Andrew J. Lew, Elia Beniash, Pupa U. P. A. Gilbert,\* and Markus J. Buehler\*



Cite This: <https://doi.org/10.1021/acsnano.1c10407>



Read Online

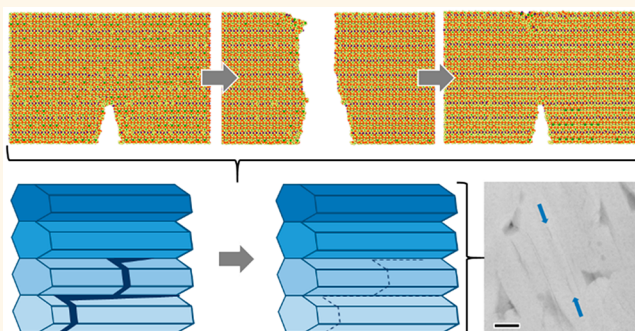
ACCESS |

Metrics & More

Article Recommendations

Supporting Information

**ABSTRACT:** Human enamel is an incredibly resilient biological material, withstanding repeated daily stresses for decades. The mechanisms behind this resilience remain an open question, with recent studies demonstrating a crack-deflection mechanism contributing to enamel toughness and other studies detailing the roles of the organic matrix and remineralization. Here, we focus on the mineral and hypothesize that self-healing of cracks in enamel nanocrystals may be an additional mechanism acting to prevent catastrophic failure. To test this hypothesis, we used a molecular dynamics (MD) approach to compare the fracture behavior of hydroxyapatite (HAP) and calcite, the main minerals in human enamel and sea urchin teeth, respectively. We find that cracks heal under pressures typical of mastication by fusion of crystals in HAP but not in calcite, which is consistent with the resilience of HAP enamel that calcite teeth lack. Scanning transmission electron microscopy (STEM) images of structurally intact (“sound”) human enamel show dashed-line nanocracks that resemble and therefore might be the cracks healed by fusion of crystals produced *in silico*. The fast, self-healing mechanism shown here is common in soft materials and ceramics but has not been observed in single crystalline materials at room temperature. The crack self-healing in sound enamel nanocrystals, therefore, is unique in the human body and unique in materials science, with potential applications in designing bioinspired materials.



**KEYWORDS:** self-healing, enamel, hydroxyapatite, calcite, molecular dynamics, simulations

Tooth enamel is the hardest and most mineralized tissue in the human body, and is the only tissue with no cells. Fully mineralized and disease-free enamel is clinically defined as sound enamel, as opposed to carious enamel. It is a nanocomposite of 95 wt% hydroxyapatite (HAP,  $\text{Ca}_5(\text{PO}_4)_3\text{OH}$ ), 1 wt % soft organic matrix, and 4 wt % water.<sup>1,2</sup> Its major function is mastication, with hundreds of masticatory cycles per day, and despite the fact that it cannot be remodeled, enamel can last a lifetime without catastrophic failure. This unique resilience of sound enamel is due to its hierarchical structure and composition.<sup>3–6</sup> It is composed of elongated HAP nanocrystals bundled into rods partly wrapped in sheaths of organic matrix and interspersed with interrod, made of similar but differently oriented HAP nanocrystals. In mammalian enamel, the rods are arranged in a complex decussating pattern, which toughens by bridging, deflecting, and bifurcating cracks.<sup>7–12</sup> This is a unique characteristic of mammalian enamel compared to other vertebrates with less resilient teeth, which replace multiple generations of teeth over their lifespan (e.g., sharks, bony fishes, amphibians, reptiles).

The unique mechanical properties of enamel has inspired the design of engineered nanomaterials.<sup>13,14</sup>

To successfully function over tens of years without catastrophic failures, enamel employs a host of mechanisms at different scales that allow it to combine high hardness and fracture toughness. Although HAP is the predominant component in enamel, organic macromolecules play significant roles in enamel toughening through ligament bridging of microcracks—several reports indicate that the organic matrix is involved in crack healing.<sup>7,10</sup> Water is also involved in enamel toughening through hydration of the organic phase.<sup>7</sup> Panda enamel, for instance, exhibits hydration-induced self-recovery due to viscoelasticity of the organic matrix.<sup>15</sup>

Received: November 24, 2021

Accepted: June 1, 2022



ACS Publications

© XXXX American Chemical Society

Despite a significant body of evidence on toughening mechanisms provided by enamel microarchitecture, organic phase, and water, very little is known about the role of the mineral. It was proposed that biological apatites are insensitive to flaws due to their nanosizes.<sup>3</sup> Our recent study<sup>16</sup> challenged a decades old paradigm that the crystals within each enamel rod are co-oriented, and that their crystalline *c*-axes are aligned with the rod axis.<sup>17–19</sup> That study, utilizing polarization-dependent imaging contrast (PIC) mapping<sup>20,21</sup> in combination with high resolution scanning electron microscopy (SEM) and transmission electron microscopy (TEM), showed that adjacent nanocrystals are actually misoriented within rods, most frequently by 1°–30°.<sup>16</sup> Upon exposure to tensile loads, bicrystals with these *c*-axis misorientations induce crack deflection, as illustrated in Figure 1a, and contribute to enamel

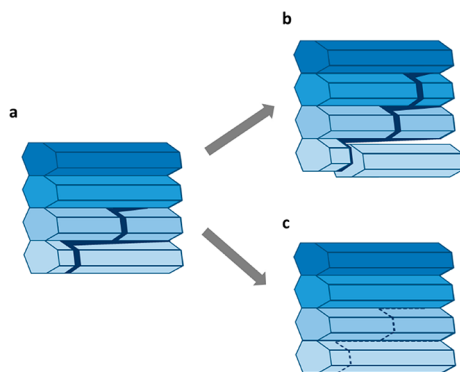


**Figure 1.** Schematic of misoriented HAP nanocrystals (crystal orientations represented with different shades of blue) within enamel rods having (a) deflected nanocrack path. Cracks typically act as (b) structural vulnerabilities weakening the material for further cracking and eventual catastrophic failure, but the long-term resilience of enamel hints at mechanisms of (c) structure regeneration attenuating the effect of nanocracks.

toughness<sup>16</sup> and hardness in various animals.<sup>22,23</sup> This perspective revealed the necessity to carefully assess the structure, orientation, and fracture behavior of crystals at the nanoscale to fully understand enamel's unique resilience at the macroscale. Specifically, it is important to investigate if cracks in individual nanocrystals can heal during mastication, and if so, how this phenomenon contributes to the macroscopic mechanical resilience of enamel. Residual cracks can accumulate over time, leading to material fatigue failure such as in Figure 1b. However, for human enamel to last for decades without catastrophic failure, we hypothesize that an alternative structure evolution may attenuate nanocrack damage as shown in Figure 1c. The HAP mineral itself is the focus of this work, where we compare how repeated fracture and compression affects the main mineral component in two different dental minerals: calcite ( $\text{CaCO}_3$ ) in sea urchin teeth, which continuously grow and self-sharpen<sup>24</sup> as pieces break off, and HAP in human enamel, adapted to last a lifetime. Specifically, we compare calcite and HAP crack healing, both in isolation and in water, to explore the role of the mineral in sound enamel.

## RESULTS/DISCUSSION

We used molecular dynamics (MD) simulations to probe repeated fracture and healing behavior of two biologically relevant minerals, calcite and HAP, present in sea urchin teeth

and human teeth's sound enamel, respectively. Figure 2a illustrates the behavior of fractured calcite and HAP nanocrystals under compression at 0.66 GPa at room temperature. This is a biologically relevant pressure, approximately what enamel is exposed to when molar teeth are clenched in the mastication processes.<sup>25,26</sup> The sources of tooth fracture are diverse,<sup>27</sup> including masticatory accidents involving suddenly biting a hard object,<sup>28</sup> defective amalgam restorations,<sup>29</sup> or even the cumulative effect of masticatory cycles in both normal and parafunction.<sup>30</sup> Here, for simplicity, fracture is induced by applying tensile loads on notched single crystals. After compression of the cracked crystals, calcite does not heal: it is left with a deformed crystal lattice and material voids along the crack. In contrast, HAP after compression heals: it reforms the original ordered lattice structure with almost no residual damage.

Atoms with fewer neighbors than their initial state in bulk, unfractured crystal are defined as dislocation or defect cores.<sup>31</sup> Quantitatively, Figure 2b shows plentiful dislocation core generation in calcite with atoms on average experiencing a 10% change in number of neighbors, notably at the significantly deformed notch tip and around persistent material voids. In contrast, HAP crack healing occurs with very little perturbation of the crystal lattice even along the fracture path, with atoms on average experiencing only a 5% change in neighbors. The details of dislocation core visualization are provided in the Methods/Experimental section and the Supporting Information.

The marked difference in behavior between calcite and HAP can be understood from an energetic perspective. Over the fracture process, new surfaces are created. The resultant structures are at a higher potential energy state, corresponding to the surface energy of the cracks, compared to the pristine crystals. We plot this change in energy for crystals of calcite and HAP in Figure 3 and find that the change in energy for calcite is much lower than for HAP. The difference in potential energies shows that HAP fracture surfaces are much less stable than calcite surfaces. This energy difference acts as an additional driving force for crack closure, resulting in HAP's markedly stronger self-healing response.

To further probe how repeated fracture and compression change crystal structures over time, the already compressed calcite and HAP nanocrystals were exposed to three additional cycles of fracture and compression. Calcite voids along the crack path grow in size with repeated fracture, leaving only minimal connection between the left and right halves of the crystal. This irreversible damage is characteristic of non-self-healing materials. In contrast, HAP continues to repeatedly fuse two crystals into a continuous single crystal, and thus, it self-heals as shown in Figure 4a. There is inevitably some resistance to repair due to energy dissipation during fracture, which manifests as mild accumulation of defects along the fracture path, but not nearly as much in HAP as in calcite.

We next repeated the study, but with the introduction of water to the system, in order to evaluate the healing mechanism in an environment similar to the mouth. For these aqueous simulations, the top and bottom free surfaces of the mineral are coated with approximately 20 Å thick layers of water molecules prior to fracture, filling the empty space in the original simulation box. We find that the presence of water can contaminate the fracture surfaces, become trapped along the crack surface upon compression, and attenuate the degree of HAP healing after repeated fracture, as shown in Figure 4b.

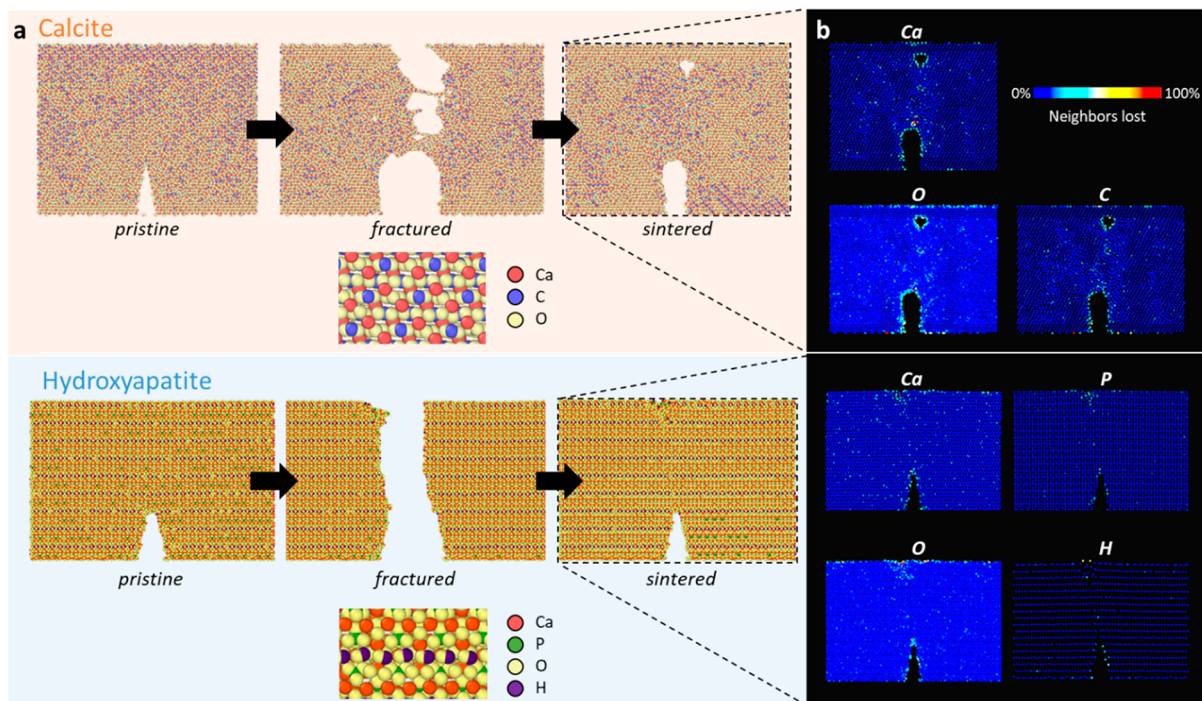


**Figure 2.** MD simulations of (a) pristine calcite and HAP nanocrystals, fractured by tensile load and compressed at typical mastication pressures, illustrate greater crack healing by fusion of crystals in HAP than in calcite. (b) Dislocations of fused crystals are displayed per element for clarity. Fracture irreversibly damages the calcite crystal lattice, resulting in the formation of material voids. In contrast, HAP cracks heal with damage limited only to scattered dislocation cores. Dislocation cores are colored according to the percentage of neighboring atoms lost over the fracture and healing processes.

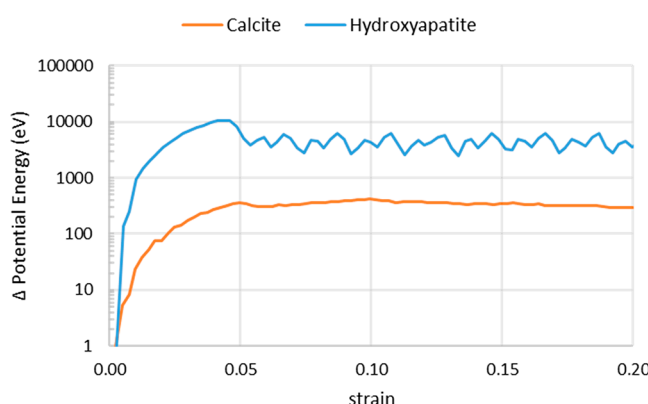


**Figure 3.** As new surfaces are created by fracture, the potential energy of both HAP and calcite crystals increases. The change in potential energy is greater for HAP than calcite, meaning that HAP surfaces are less stable than calcite surfaces. This difference in potential energy acts as an additional driving force for the elimination of HAP fracture surfaces, resulting in the difference in self-healing behavior between the two crystals.

Despite this, the comparison of HAP to calcite still favors HAP, with crack healing behavior again present in HAP but not in calcite.

To evaluate the consistency of our simulated results with reality, we experimentally imaged sound human enamel from a healthy young adult molar, as presented in Figure 4c. Thin crack features with various line widths and lengths were observed with scanning transmission electron microscopy (STEM). In some areas, adjacent cracks are observed within 5 nm of each other, much closer than the smallest enamel crystal widths of 15 nm.<sup>32</sup> Thus, these lines are consistent with

cracks within HAP crystals, rather than being intercrystal features such as grain boundaries. Additionally, these lines cannot correspond to the well-known central dark line (CDL) in each enamel HAP nanocrystal.<sup>33</sup> This is because, under the annular dark field detectors used to obtain better CDL detection than regular high resolution TEM, CDLs visually appear as brighter lines due to the higher z-contrast.<sup>34–36</sup> Our micrographs are acquired in the same way; hence, the dark lines we observed are not CDLs. These intracrystal nanocracks sometimes completely disappear before reappearing further along the same path and thus appear as dashed lines. It is impossible to determine if these dashed lines are the result of previously bigger cracks that healed or incipient cracks that would have grown bigger if the donor had continued to chew on them. If the observed dashed lines are a result of crack healing within HAP crystals, then nanocracks disappeared where healed and persisted where not healed (perhaps due to similar surface contamination mechanisms as identified in Figure 4b). Other than the presence of dashed-line nanocracks, the structure of the enamel in Figure 4c is perfectly intact. Thus, dashed-line damage is below the threshold for causing catastrophic failure during the life of the donor.

We investigate the self-healing behavior of HAP in aqueous environment in further detail with Figure 5a, which indicates that HAP outperforms calcite in ultimate fracture strength over all repeated fractures. Strikingly, the efficacy of HAP healing is demonstrated in how the strength of healed HAP after one fracture is comparable to and slightly higher than the strength of pristine calcite. Additionally, the sample toughness calculated as the area under the stress strain curve<sup>37</sup> also demonstrates the effectiveness of HAP healing in Figure 5b. Here, the decrease in toughness between the first and second

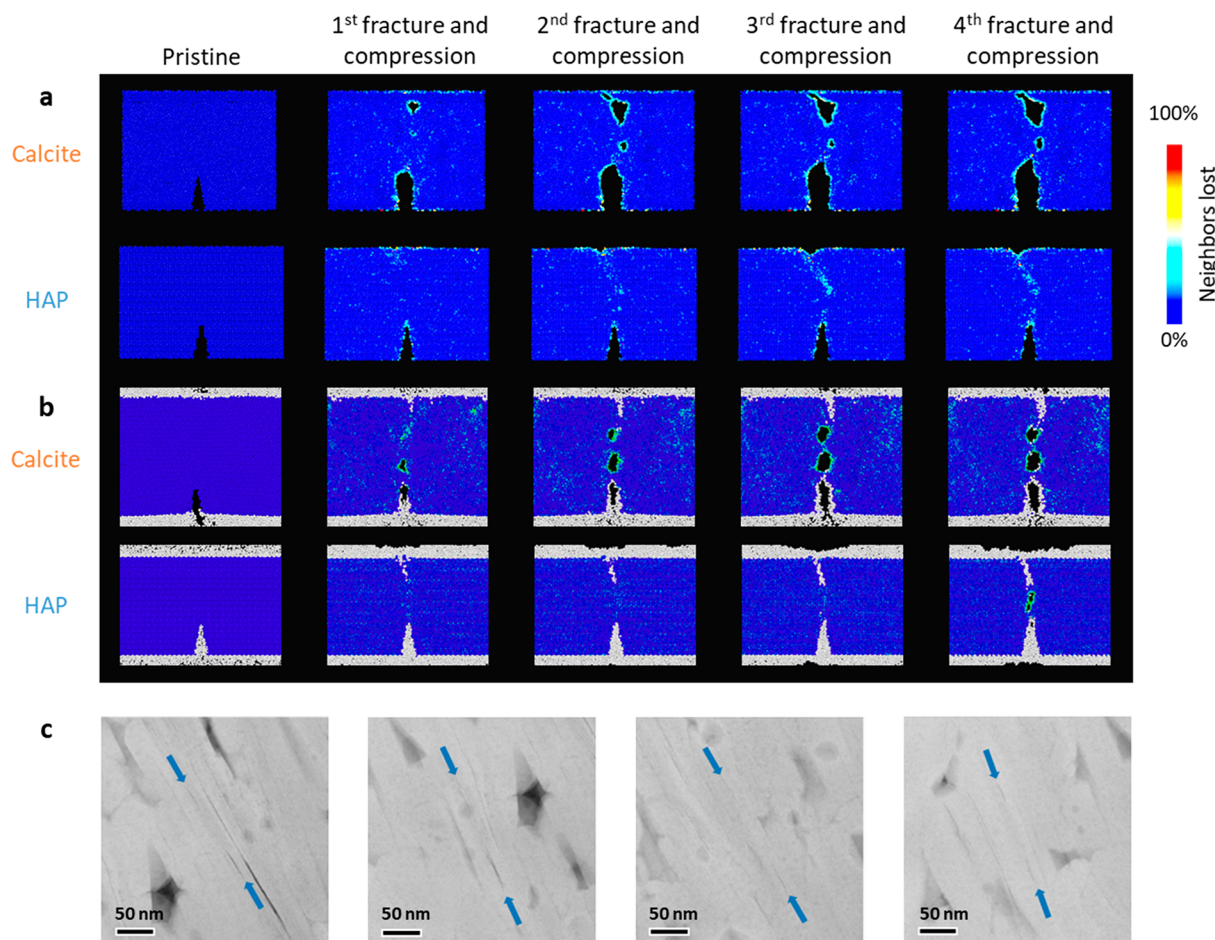


**Figure 4.** Over repeated cycles of fracture and compression, (a) the calcite nanocrystal is irreparably damaged with large persistent gaps formed along the fracture path, while the HAP nanocrystal is healed with comparatively minor generation of dislocation cores along the fracture path. (b) While the introduction of water (light gray atoms at top, bottom, and within the cracks of the crystal) contaminates the crack surface and attenuates HAP healing after repeated fracture, the comparative observation of greater residual damage in calcite than HAP still holds. (c) STEM images of HAP in human enamel reveal hairline cracks that vary in width, sometimes completely disappearing before reappearing further down the material. Such dashed lines are shown in four panels between pairs of arrowheads. Distances between parallel cracks can reach <5 nm, too close to be grain boundaries between adjacent HAP crystals. Dashed-line nanocracks within HAP crystals may be partly healed cracks.

fractures is much greater for calcite than HAP, with the difference due to the ability for HAP to recover a degree of its mechanical properties by crack healing. On average, calcite loses 49% of its toughness after fracture while HAP only loses 33%. After enough repeated fracture, both tensile strength and toughness of HAP degrade to levels comparable to those of calcite, illustrating an operational limit to the crack healing process.

## CONCLUSIONS

MD simulations reveal very different crack healing behaviors of calcite and HAP after fracture and compression. Calcite crystals remain irreversibly damaged under biological compression conditions, with persistent material voids that only grow in size with repeated loading. Such irreparable damage to a major dental component is of little concern to organisms with the ability to continuously grow teeth, such as sea urchins. In contrast, human enamel must last a lifetime and natural selection would favor a dental material minimizing fracture vulnerability. The ability for HAP nanocracks to self-heal under compression may significantly contribute to sound enamel's long-term resilience.

Self-healing of cracks in crystals is not a unique concept—studies on crack healing in inorganic ceramic materials date back to the 1960s.<sup>38</sup> Since then, various metal oxides and silicon compounds have been identified, taking advantage of both local sintering and oxidation reaction pathways<sup>39,40</sup> to heal microcracks. Recently, so-called MAX phase compounds<sup>41</sup> have been studied for their ability to fully and repeatedly self-heal. In particular, Ti<sub>2</sub>AlC has experimentally demonstrated similar behavior to our HAP results - initial microcrack healing is robust enough for a second microcrack to take a different fracture path, with subsequent cracking exhibiting decreased degrees of healing.<sup>42</sup>

However, notable differences make the HAP case unique, despite bearing similarities in repeated fracture behavior and the mechanism of crystal fusion under compression. First, the chemical composition of HAP is not a metal oxide, silicon-based, or a MAX phase. Second, HAP crack healing is simulated to occur at room temperature instead of the 1000 K temperatures common for MAX phases. To our knowledge, compression-based crack healing has not been observed at room temperature. Third, and perhaps the reason for the first two differences, we have identified healing at the nanoscale

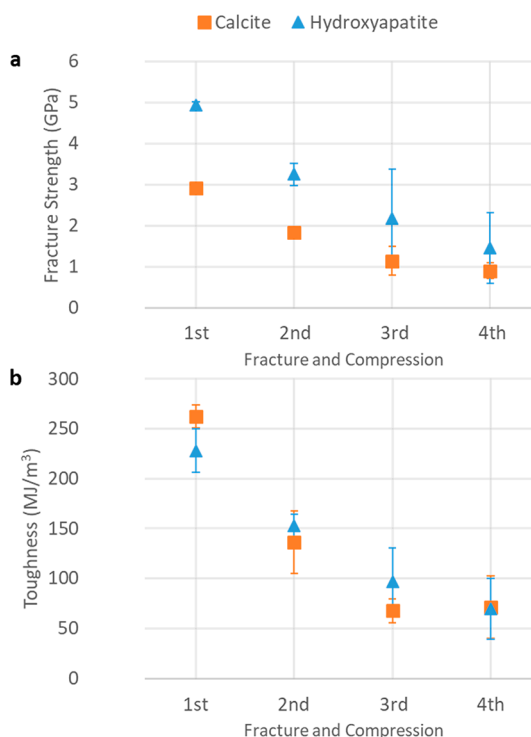


**Figure 5.** Quantitative comparison of aqueous calcite and aqueous HAP crystal fracture demonstrates that (a) the repeated fracture strength of HAP is consistently 67% greater than that of calcite, with the first fracture strength of pristine calcite slightly lower than the second fracture strength of HAP. (b) Additionally, the decrease in material toughness between subsequent fractures and compressions is much less pronounced for HAP than for calcite—on average HAP only loses 33%, while calcite loses 49% of its toughness.

rather than microscale. The nanoscale nature of our system may be a contributing factor as to why crack healing is observed at low temperature: high surface energy to volume ratio at the nanoscale may drive healing at comparatively mild conditions.

Another relevant aspect of the healing process observed in MD simulations is the time it takes to heal a crack. We consistently observed crack healing within 10 ps. Such fast healing is essential in as dynamic a system as teeth during mastication: if a nanocrack did not heal immediately, its two sides may be displaced with respect to one another, leading to structural modification and loss of function. HAP fast crack healing is appealing for bioinspired robotic materials.<sup>43,44</sup>

Finally, HAP self-healing may explain the formation mechanism of another thus far unexplained enamel structure. Unerupted teeth possess a loosely packed surface enamel structure distinct from mature erupted teeth. This porous surface enamel exists up to the time of eruption. Then, it begins losing porosity as a function of time after eruption.<sup>45</sup> The surface enamel eventually becomes identical with the closely packed crystals of subsurface enamel.<sup>46</sup> But, the mechanism by which this change occurs is not known. In light of our HAP results, mastication forces after eruption may facilitate the fusion of enamel crystals and could contribute to this structural change.

Future work may include more thorough experimental studies of fracture evolution in enamel, by the analysis of tooth samples with known degrees of failure and stress history.

Additionally, further complexity in the MD model to incorporate effects of bond breakage with reactive force fields, inclusions of natural chemical impurities in the crystal lattices, and organics will allow us to go beyond mechanism identification and assist the development of a more quantitative, general model for biomimetic failure, healing, and design.

## METHODS/EXPERIMENTAL

**MD Simulations of Fracture and Fusion of Crystals.** All simulations were run on computer clusters at NERSC and at MIT. We used an MD approach from previous studies of calcite<sup>47</sup> and HAP<sup>16,48–50</sup> utilizing LAMMPS<sup>51</sup> to probe the behavior of repeated nanocrystal fracture. Here, we chose a system periodic in width and depth and measuring 15 nm high as a representative HAP nanocrystal. This 15 nm dimension is on the order of the HAP subunits observed in mature human enamel<sup>52</sup> and on the low end of the distribution of observed enamel crystal thicknesses.<sup>32</sup> Taking this smaller system size is intentional for computational expediency while still capturing a physically relevant size. Calcite nanocrystals of comparable size were chosen to make a direct comparison.

A triangular 5 nm deep  $\times$  2 nm wide surface notch was introduced at the bottom center of each crystal as an initial crack before exposure to tensile loads. Initial surface notches were created by deleting atoms within the notch region while both maintaining charge neutrality and without leaving partial phosphate or carbonate ions. After notching, these HAP and calcite crystals were composed of 23,333 and 24,450 atoms, respectively. Simulation conditions used the NPT ensemble at 300 K. A strain rate of 1 m/s, up to strain of 0.2, was used to fracture the sample. Crystal halves were subsequently brought back together and compressed to 0.66 GPa over 10 ps. This was held at 0.66 GPa for 10 ps to make the two halves fuse, before returning the pressure to 1 atm over a subsequent 10 ps. Finally, the sample was held at 1 atm for 10 ps before being subject to subsequent fracture. Three separate HAP simulation runs, each consisting of four fracture and compression cycles, were performed to gather a general representation of fracture behavior over different thermal fluctuations. Calculations of the stress tensor<sup>53</sup> were performed within LAMMPS and averaged across the three runs to provide the values in Figure 5, with error bars representing the standard deviation. The mechanical behavior of HAP nanocrystals was validated against previous studies<sup>16</sup> with close agreement in fracture strain. A fractional difference in yield strength compared to larger sample sizes is expected and may be attributed to the size effect reducing the free path for dislocation movement.<sup>54</sup>

**Visualizations of MD Simulations.** Visualization of atomic structure and crystal defects at various timesteps were done in OVITO.<sup>55</sup> Coloration was done by a revised coordination number analysis<sup>31</sup> due to the method's ease of use and independence from the choice of force field. Due to the crystal structures of calcite and HAP consisting of multiple interpenetrating elemental lattices, a typical coordination number such as 12 for FCC or 8 for BCC is not used. Instead custom neighbor cutoff radii of 5.2 Å for calcite and 4 Å for HAP are chosen in order to capture relevant interatomic interaction distances. Further detail is provided in the Supporting Information.

**Energy Calculations of Fractured Crystals.** Material toughness is the ability for a material to absorb energy during deformation, measured by calculating the area under the stress strain curve from a tensile test, with units of energy per volume of material.<sup>37</sup> Specifically, this is shown in the following eq 1:

$$T = \int_0^{\varepsilon_f} \sigma d\varepsilon \quad (1)$$

where  $T$  is toughness,  $\sigma$  is the stress,  $\varepsilon$  is the strain, and  $\varepsilon_f$  is the final strain. Integrating the area under the stress strain curve multiplies the units of stress (Pa) by the units of strain (unitless), providing units of  $\text{Pa} = \text{N}/\text{m}^2 = \text{N}\cdot\text{m}/\text{m}^3 = \text{J}/\text{m}^3$ , i.e., energy per volume.

Fracture toughness is a separate value from material toughness that represents the energy needed to fracture a material from an initial

notch, with units of MPa·m<sup>1/2</sup>.<sup>56</sup> As our simulations are subject to periodic boundary conditions, the samples under investigation can be considered to have infinite thickness. Thus, we are in the case of plane strain,<sup>56</sup> and fracture toughness can be approximated according to the following eq 2:

$$K_c = \sigma \sqrt{\pi a} \quad (2)$$

where  $K_c$  is the fracture toughness,  $\sigma$  is the stress, and  $a$  is the notch length. For a given initial notch size, materials that can withstand a greater stress before fracture have a greater fracture toughness.

Another measure of fracture resistance can be derived from the amount of energy required to grow a crack during fracture, with units of energy per area of crack surface.<sup>57</sup> This critical energy release rate can be approximated as the following eq 3:

$$G_c = \frac{\sigma_f^2 \pi a}{E} \quad (3)$$

where  $G_c$  is the critical energy release rate,  $\sigma_f$  is the failure stress,  $a$  is the crack length, and  $E$  is the Young's modulus. These latter two material properties are plotted in the Supporting Information as Figure S3 and show good agreement with the literature.<sup>58–60</sup>

**Focused Ion Beam (FIB) Preparation of Enamel Samples.** The FIB sections of human dental enamel were prepared as described in Beniash et al.<sup>16</sup> Briefly, a deidentified third mandibular molar extracted for orthodontic purposes was collected at the Dept. of Oral and Maxillofacial Surgery, University of Pittsburgh School of Dental Medicine. The coronal portion of the tooth was separated from the roots and sectioned into 200  $\mu\text{m}$  thick sections in the mesio-distal plane. The preparation of the FIB samples was conducted using a 1540XB CrossBeam Zeiss Auriga FIB field emission SEM, equipped with a Ga liquid metal ion source at the Nanoscale Imaging and Analysis Center (NIAC), University of Wisconsin-Madison. The FIB samples were prepared in such a way that the rods were all parallel to each other and oriented in the plane of the section. The enamel samples were 100 nm thick and 20  $\mu\text{m} \times 100 \mu\text{m}$  wide.

**STEM of Enamel Samples.** The enamel samples were studied at the University of Pittsburgh Nanoscale Fabrication and Characterization Facility (NFCF), using a FEI Titan Themis G2 200 Probe Cs Corrected STEM at 200 kV acceleration voltage.

## ASSOCIATED CONTENT

### Supporting Information

The Supporting Information is available free of charge at <https://pubs.acs.org/doi/10.1021/acsnano.1c10407>.

Details on MD crystal equilibration, defect visualization, and fracture property calculations ([PDF](#))

## AUTHOR INFORMATION

### Corresponding Authors

○ Pupa U. P. A. Gilbert – Department of Physics, University of Wisconsin, Madison, Wisconsin 53706, United States; Departments of Chemistry, Materials Science and Engineering, Geoscience, University of Wisconsin, Madison, Wisconsin 53706, United States; Chemical Sciences Division, Lawrence Berkeley National Laboratory, Berkeley, California 94720, United States; [orcid.org/0000-0002-0139-2099](#); Email: [pupa@physics.wisc.edu](mailto:pupa@physics.wisc.edu)

Markus J. Buehler – Laboratory for Atomistic and Molecular Mechanics (LAMM), Massachusetts Institute of Technology, Cambridge, Massachusetts 02139, United States; Center for Computational Science and Engineering, Schwarzman College of Computing, Massachusetts Institute of Technology, Cambridge, Massachusetts 02139, United States; [orcid.org/0000-0002-4173-9659](#); Email: [mbuehler@mit.edu](mailto:mbuehler@mit.edu)

## Authors

Andrew J. Lew – Laboratory for Atomistic and Molecular Mechanics (LAMM), Massachusetts Institute of Technology, Cambridge, Massachusetts 02139, United States; Department of Chemistry, Massachusetts Institute of Technology, Cambridge, Massachusetts 02139, United States; [orcid.org/0000-0002-4072-114X](#)

Elia Beniash – Departments of Oral Biology and Bioengineering, Center for Craniofacial Regeneration, McGowan Institute for Regenerative Medicine, University of Pittsburgh, Pittsburgh, Pennsylvania 15260, United States; [orcid.org/0000-0001-9019-5160](#)

Complete contact information is available at:

<https://pubs.acs.org/10.1021/acsnano.1c10407>

## Author Contributions

P.U.P.A.G. conceived the ideas that human enamel nanocrystals may be self-healing and that MD simulations could demonstrate it, M.J.B. and A.J.L. designed the MD simulations to test this hypothesis, A.J.L. performed the MD simulations, and E.B. acquired the STEM data. A.J.L. and M.J.B. analyzed the MD data and all authors discussed the results in the broader context of experiment and simulation. A.J.L. and P.U.P.A.G. wrote the manuscript and M.J.B. and E.B. edited it.

## Notes

The authors declare no competing financial interest.

○ Previously publishing as Gelsomina De Stasio

## ACKNOWLEDGMENTS

The authors would like to thank Dr. G. S. Jung for discussions, C. A. Stifler for embedding and polishing the human tooth, and R. Noll for FIBing it. A.J.L. acknowledges support from National Science Foundation (NSF) grant No. 1122374. Any opinion, findings, and conclusions or recommendations expressed in this material are those of the authors and do not necessarily reflect the views of the NSF. The authors thank the National Energy Research Scientific Computing Center (NERSC) at Lawrence Berkeley National Laboratory for cluster computing time awarded to project m3650. E.B. acknowledges support from National Institute of Dental and Craniofacial Research (NIH/NIDCR) under award R21DE029604. The authors acknowledge the Nanoscale Fabrication & Characterization Facility at the University of Pittsburgh and Dr. Stephen House for help with STEM microscopy. P.U.P.A.G. acknowledges 80% support from the U.S. Department of Energy, Office of Science, Office of Basic Energy Sciences, Chemical Sciences, Geosciences, and Biosciences Division, under Awards DE-FG02-07ER15899 and FP0001113S, and 20% support from NSF grant DMR-1603192. M.J.B. and A.J.L. acknowledge support from ONR (N000141612333 and N000141912375) and AFOSR (FATE MURI FA9550-15-1-0514), as well as NIH U01HH4977, U01EB014976, and U01EB016422.

## REFERENCES

- (1) Fincham, A. G.; Moradian-Oldak, J.; Simmer, J. P. The Structural Biology of the Developing Dental Enamel Matrix. *J. Struct. Biol.* **1999**, 126 (3), 270–299.
- (2) Lacruz, R. S.; Habelitz, S.; Wright, J. T.; Paine, M. L. Dental Enamel Formation and Implications for Oral Health and Disease. *Physiol. Rev.* **2017**, 97 (3), 939–993.

- (3) Gao, H.; Ji, B.; Jäger, I. L.; Arzt, E.; Fratzl, P. Materials Become Insensitive to Flaws at Nanoscale: Lessons from Nature. *Proc. Natl. Acad. Sci. U. S. A.* **2003**, *100* (10), 5597–5600.
- (4) Chai, H.; Lee, J. J. W.; Constantino, P. J.; Lucas, P. W.; Lawn, B. R. Remarkable Resilience of Teeth. *Proc. Natl. Acad. Sci. U. S. A.* **2009**, *106* (18), 7289–7293.
- (5) Lawn, B. R.; Lee, J. J.-W.; Chai, H. Teeth: Among Nature's Most Durable Biocomposites. *Annu. Rev. Mater. Res.* **2010**, *40* (1), 55–75.
- (6) Wilmers, J.; Bargmann, S. Nature's Design Solutions in Dental Enamel: Uniting High Strength and Extreme Damage Resistance. *Acta Biomater.* **2020**, *107*, 1–24.
- (7) Baldassarri, M.; Margolis, H. C.; Beniash, E. Compositional Determinants of Mechanical Properties of Enamel. *J. Dent. Res.* **2008**, *87* (7), 645–649.
- (8) Bajaj, D.; Nazari, A.; Eidelman, N.; Arola, D. D. A Comparison of Fatigue Crack Growth in Human Enamel and Hydroxyapatite. *Biomaterials* **2008**, *29* (36), 4847–4854.
- (9) Bajaj, D.; Arola, D. Role of Prism Decussation on Fatigue Crack Growth and Fracture of Human Enamel. *Acta Biomater.* **2009**, *5* (8), 3045–3056.
- (10) Bajaj, D.; Arola, D. D. On the R-Curve Behavior of Human Tooth Enamel. *Biomaterials* **2009**, *30* (23–24), 4037–4046.
- (11) Rivera, C.; Arola, D.; Ossa, A. Indentation Damage and Crack Repair in Human Enamel. *J. Mech. Behav. Biomed. Mater.* **2013**, *21*, 178–184.
- (12) Yahyazadehfar, M.; Arola, D. The Role of Organic Proteins on the Crack Growth Resistance of Human Enamel. *Acta Biomater.* **2015**, *19*, 33–45.
- (13) Yeom, B.; Sain, T.; Lacevic, N.; Bukharina, D.; Cha, S. H.; Waas, A. M.; Arruda, E. M.; Kotov, N. A. Abiotic Tooth Enamel. *Nature* **2017**, *543* (7643), 95–98.
- (14) Zhao, H.; Liu, S.; Wei, Y.; Yue, Y.; Gao, M.; Li, Y.; Zeng, X.; Deng, X.; Kotov, N. A.; Guo, L.; Jiang, L. Multiscale Engineered Artificial Tooth Enamel. *Science* **2022**, *375* (6580), 551–556.
- (15) Liu, Z.; Weng, Z.; Zhai, Z. F.; Huang, N.; Zhang, Z. J.; Tan, J.; Jiang, C.; Jiao, D.; Tan, G.; Zhang, J.; Jiang, X.; Zhang, Z.; Ritchie, R. O. Hydration-Induced Nano- to Micro-Scale Self-Recovery of the Tooth Enamel of the Giant Panda. *Acta Biomater.* **2018**, *81*, 267–277.
- (16) Beniash, E.; Stifler, C. A.; Sun, C. Y.; Jung, G. S.; Qin, Z.; Buehler, M. J.; Gilbert, P. U. P. A. The Hidden Structure of Human Enamel. *Nat. Commun.* **2019**, *10* (1), 1–13.
- (17) Nylen, M. U.; Eanes, E. D.; Omnell, K. A. Crystal Growth in Rat Enamel. *J. Cell Biol.* **1963**, *18* (1), 109–123.
- (18) Travis, D. F.; Glimcher, M. J. The Structure and Organization of, and the Relationship between the Organic Matrix and the Inorganic Crystals of Embryonic Bovine Enamel. *J. Cell Biol.* **1964**, *23* (3), 447–497.
- (19) Glimcher, M. J.; Daniel, E. J.; Travis, D. F.; Kamhi, S. Electron Optical and X-Ray Diffraction Studies of the Organization of the Inorganic Crystals in Embryonic Bovine Enamel. *J. Ultrasucture Res.* **1965**, *12*, 1–77.
- (20) Gilbert, P. U. P. A.; Young, A.; Coppersmith, S. N. Measurement of C-Axis Angular Orientation in Calcite ( $\text{CaCO}_3$ ) Nanocrystals Using X-Ray Absorption Spectroscopy. *Proc. Natl. Acad. Sci. U. S. A.* **2011**, *108* (28), 11350–11355.
- (21) Devol, R. T.; Metzler, R. A.; Kabalah-Amitai, L.; Pokroy, B.; Politi, Y.; Gal, A.; Addadi, L.; Weiner, S.; Fernandez-Martinez, A.; Demichelis, R.; Gale, J. D.; Ihli, J.; Meldrum, F. C.; Blonsky, A. Z.; Killian, C. E.; Salling, C. B.; Young, A. T.; Marcus, M. A.; Scholl, A.; Doran, A.; Jenkins, C.; Bechtel, H. A.; Gilbert, P. U. P. A. Oxygen Spectroscopy and Polarization-Dependent Imaging Contrast (PIC)-Mapping of Calcium Carbonate Minerals and Biominerals. *J. Phys. Chem. B* **2014**, *118* (28), 8449–8457.
- (22) Stifler, C. A.; Jakes, J. E.; North, J. D.; Green, D. R.; Weaver, J. C.; Gilbert, P. U. P. A. Crystal Misorientation Correlates with Hardness in Tooth Enamels. *Acta Biomater.* **2021**, *120*, 124–134.
- (23) Stifler, C. A.; Wittig, N. K.; Sassi, M.; Sun, C. Y.; Marcus, M. A.; Birkedal, H.; Beniash, E.; Rosso, K. M.; Gilbert, P. U. P. A. X-Ray Linear Dichroism in Apatite. *J. Am. Chem. Soc.* **2018**, *140* (37), 11698–11704.
- (24) Killian, C. E.; Metzler, R. A.; Gong, Y.; Churchill, T. H.; Olson, I. C.; Trubetskoy, V.; Christensen, M. B.; Fournelle, J. H.; De Carlo, F.; Cohen, S.; Mahamid, J.; Scholl, A.; Young, A.; Doran, A.; Wilt, F. H.; Coppersmith, S. N.; Gilbert, P. U. P. A. Self-Sharpening Mechanism of the Sea Urchin Tooth. *Adv. Funct. Mater.* **2011**, *21* (4), 682–690.
- (25) Dejak, B.; Młotkowski, A.; Romanowicz, M. Finite Element Analysis of Stresses in Molars during Clenching and Mastication. *J. Prosthet. Dent.* **2003**, *90* (6), 591–597.
- (26) Varga, S.; Spalj, S.; Lapter Varga, M.; Anic Milosevic, S.; Mestrovic, S.; Slaj, M. Maximum Voluntary Molar Bite Force in Subjects with Normal Occlusion. *Eur. J. Orthod.* **2011**, *33* (4), 427–433.
- (27) Gonzalez-Guajardo, D. I.; Ramirez-Herrera, G. M.; Mas-Enriquez, A.; Capetillo-Hernandez, G. R.; Tiburcio-Morteo, L.; Cabral-Romero, C.; Hernandez-Delgadillo, R.; Solis-Soto, J. M. Cracked Tooth Syndrome, an Update. *Int. J. Appl. Dent. Sci.* **2021**, *7* (2), 314–317.
- (28) Rosen, H. Cracked Tooth Syndrome. *J. Prosthet. Dent.* **1982**, *47* (1), 36–43.
- (29) Lubisich, E. B.; Hilton, T. J.; Ferracane, J. Cracked Teeth: A Review of the Literature. *J. Esthet. Restor. Dent.* **2010**, *22* (3), 158–167.
- (30) Bhandari, S. Facts About Cracks in Teeth. *Prim. Dent. J.* **2021**, *10* (1), 20–27.
- (31) Li, D.; Wang, F.; Yang, Z.; Zhao, Y. How to Identify Dislocations in Molecular Dynamics Simulations? *Sci. China-Phys. Mech Astron.* **2014**, *57*, 2177–2187.
- (32) Frazier, P. D. Adult Human Enamel: An Electron Microscopic Study of Crystallite Size and Morphology. *J. Ultrasucture Res.* **1968**, *22* (1–2), 1–11.
- (33) Yanagisawa, T.; Miake, Y. High-Resolution Electron Microscopy of Enamel-Crystal Demineralization and Remineralization in Carious Lesions. *J. Electron Microsc. (Tokyo)* **2003**, *S2* (6), 605–613.
- (34) Gasga, J. R.; Carbajal-De-La-Torre, G.; Bres, E.; Gil-Chavarria, I. M.; Rodriguez-Hernández, A. G.; Garcia-Garcia, R. STEM-HAADF Electron Microscopy Analysis of the Central Dark Line Defect of Human Tooth Enamel Crystallites. *J. Mater. Sci. Mater. Med.* **2008**, *19* (2), 877–882.
- (35) Reyes-Gasga, J.; Hémmerlé, J.; Brès, E. F. Aberration-Corrected Transmission Electron Microscopic Study of the Central Dark Line Defect in Human Tooth Enamel Crystals. *Microsc. Microanal.* **2016**, *22*, 1047–1055.
- (36) DeRocher, K. A.; Smeets, P. J. M.; Goodge, B. H.; Zachman, M. J.; Balachandran, P. V.; Stegbauer, L.; Cohen, M. J.; Gordon, L. M.; Rondinelli, J. M.; Kourkoutis, L. F.; Joester, D. Chemical Gradients in Human Enamel Crystallites. *Nat. 2020 5837814* **2020**, *583* (7814), 66–71.
- (37) Callister, W. D.; Rethwisch, D. G. Chapter 6 Mechanical Properties of Metals. In *Materials Science and Engineering: An Introduction*, 7th ed.; John Wiley & Sons, Inc: New York, NY, 2013; pp 131–173.
- (38) Heuer, A.; Roberts, J. The Influence of Annealing on the Strength of Corundum Crystals. *Proc. Br. Ceram. Soc.* **1966**, *6*, 17–27.
- (39) Li, S.; Song, G.; Kwakernaak, K.; van der Zwaag, S.; Sloof, W. G. Multiple Crack Healing of a  $\text{Ti}_2\text{AlC}$  Ceramic. *J. Eur. Ceram. Soc.* **2012**, *32* (8), 1813–1820.
- (40) Li, S.; Bei, G.; Chen, X.; Zhang, L.; Zhou, Y.; Mačković, M.; Speicker, E.; Greil, P. Crack Healing Induced Electrical and Mechanical Properties Recovery in a  $\text{Ti}_2\text{SnC}$  Ceramic. *J. Eur. Ceram. Soc.* **2016**, *36* (1), 25–32.
- (41) Radovic, M.; Barsoum, M. W. MAX Phases: Bridging the Gap between Metals and Ceramics. *Am. Ceram. Soc. Bull.* **2013**, *92* (3), 20–27.
- (42) Sloof, W. G.; Pei, R.; McDonald, S. A.; Fife, J. L.; Shen, L.; Boatemaa, L.; Farle, A. S.; Yan, K.; Zhang, X.; Van Der Zwaag, S.; Lee, P. D.; Withers, P. J. Repeated Crack Healing in MAX-Phase Ceramics

Revealed by 4D In Situ Synchrotron X-Ray Tomographic Microscopy.

*Sci. Rep.* **2016**, *6* (1), 1–9.

(43) Pena-Francesch, A.; Jung, H.; Demirel, M. C.; Sitti, M. Biosynthetic Self-Healing Materials for Soft Machines. *Nat. Mater.* **2020**, *19*, 1230–1235.

(44) Speck, T.; Mülhaupt, R.; Speck, O. Self-Healing in Plants as Bio-Inspiration for Self-Repairing Polymers. In *Self-Healing Polymers*; Wiley-VCH Verlag GmbH & Co. KGaA: Weinheim, Germany, 2013; pp 61–89.

(45) Palamara, J.; Phakey, P. P.; Rachinger, W. A.; Orams, H. J. Electron Microscopy of Surface Enamel of Human Unerupted and Erupted Teeth. *Arch. Oral Biol.* **1980**, *25* (11–12), 715–725.

(46) Crabb, H. S. M. The Porous Outer Enamel of Unerupted Human Premolars. *Caries Res.* **1976**, *10* (1), 1–7.

(47) Raiteri, P.; Demichelis, R.; Gale, J. D. Thermodynamically Consistent Force Field for Molecular Dynamics Simulations of Alkaline-Earth Carbonates and Their Aqueous Speciation. *J. Phys. Chem. C* **2015**, *119* (43), 24447–24458.

(48) Nair, A. K.; Gautieri, A.; Chang, S. W.; Buehler, M. J. Molecular Mechanics of Mineralized Collagen Fibrils in Bone. *Nat. Commun.* **2013**, *4* (1), 1–9.

(49) Nair, A. K.; Gautieri, A.; Buehler, M. J. Role of Intrafibrillar Collagen Mineralization in Defining the Compressive Properties of Nascent Bone. *Biomacromolecules* **2014**, *15* (7), 2494–2500.

(50) Depalle, B.; Qin, Z.; Shefelbine, S. J.; Buehler, M. J. Large Deformation Mechanisms, Plasticity, and Failure of an Individual Collagen Fibril With Different Mineral Content. *J. Bone Miner. Res.* **2016**, *31* (2), 380–390.

(51) Plimpton, S. Fast Parallel Algorithms for Short-Range Molecular Dynamics. *J. Comput. Phys.* **1995**, *117* (1), 1–19.

(52) Robinson, C.; Connell, S. D. Crystal Initiation Structures in Developing Enamel: Possible Implications for Caries Dissolution of Enamel Crystals. *Front. Physiol.* **2017**, *8* (JUN), 405.

(53) Thompson, A. P.; Plimpton, S. J.; Mattson, W. General Formulation of Pressure and Stress Tensor for Arbitrary Many-Body Interaction Potentials under Periodic Boundary Conditions. *J. Chem. Phys.* **2009**, *131* (15), 154107.

(54) Wang, J.; Shaw, L. L. Nanocrystalline Hydroxyapatite with Simultaneous Enhancements in Hardness and Toughness. *Biomaterials* **2009**, *30* (34), 6565–6572.

(55) Stukowski, A. Visualization and Analysis of Atomistic Simulation Data with OVITO—the Open Visualization Tool. *Model. Simul. Mater. Sci. Eng.* **2010**, *18* (1), 015012.

(56) Callister, W. D.; Rethwisch, D. G. Chapter 8 Failure. In *Materials Science and Engineering: An Introduction*, 7th ed.; John Wiley & Sons, Inc: New York, NY, 2013; pp 207–251.

(57) Griffith, A. A. VI. The Phenomena of Rupture and Flow in Solids. *Philos. Trans. R. Soc. London. Ser. A, Contain. Pap. a Math. or Phys. Character* **1921**, *221*, 163–198.

(58) Ravaglioli, A.; Krajewski, A. *Bioceramics: Materials, Properties, Applications*, 1st ed.; Chapman & Hall: Faenza, Italy, 1992.

(59) White, S. N.; Luo, W.; Paine, M. L.; Fong, H.; Sarikaya, M.; Snead, M. L. Biological Organization of Hydroxyapatite Crystallites into a Fibrous Continuum Toughens and Controls Anisotropy in Human Enamel. *J. Dent. Res.* **2001**, *80* (1), 321–326.

(60) Saber-Samandari, S.; Gross, K. A. Micromechanical Properties of Single Crystal Hydroxyapatite by Nanoindentation. *Acta Biomater.* **2009**, *5* (6), 2206–2212.